PROCEEDINGS OF SCIENCE

Prospects for $K^+ \to \pi^+ \nu\bar{\nu}$ observation at CERN

Polenkevich Irina[*†]
JINR, Dubna (Russia)
E-mail: irinalexpol@mail.ru

The rare decays $K^+ \to \pi^+ \nu\bar{\nu}$ are excellent tool to make tests of new physics complementary to LHC thanks to their theoretically cleanness. The NA62 experiment at CERN SPS aims to collect of the order of 100 $K^+ \to \pi^+ \nu\bar{\nu}$ events in two years of data taking, keeping the background at the level of 10%. Part of the experimental apparatus has been commissioned during the technical run in 2012. The physics prospects and status of the experiment will be reviewed.

The XXI International Workshop High Energy Physics and Quantum Field Theory,
June 23 - June 30, 2013
Saint Petersburg Area, Russia

[*]Speaker.

[†]for the NA62 Collaboration: G. Aglieri Rinella, F. Ambrosino, B. Angelucci, A. Antonelli, G. Anzivino, R. Arcidiacono, I. Azhinenko, S. Balev, A. Biagioni, C. Biino, A. Bizzeti, T. Blazek, A. Blik, B. Bloch-Devaux, V. Bolotov, V. Bonaiuto, D. Britton, G. Britvich, N. Brook, F. Bucci, V. Buescher, F. Butin, T. Capussela, V. Carassiti, N. Cartiglia, A. Cassese, A. Catinaccio, A. Ceccucci, P. Cenci, V. Cerny, C. Cerri, O. Chikilev, R. Ciaranfi, G. Collazuol, P. Cooke, P. Cooper, E. Cortina Gil, F. Costantini, A. Cotta Ramusino, D. Coward, G. D'Agostini, J. Dainton, P. Dalpiaz, H. Danielsson, N. De Simone, D. Di Filippo, L. Di Lella, N. Doble, V. Duk, V. Elsha, J. Engelfried, V. Falaleev, R. Fantechi, L. Federici, M. Fiorini, J. Fry, A. Fucci, S. Gallorini, L. Gatignon, A. Gianoli, S. Giudici, L. Glonti, F. Gonnella, E. Goudzovski, R. Guida, E. Gushchin, F. Hahn, B. Hallgren, H. Heath, F. Herman, E. Iacopini, O. Jamet, P. Jarron, K. Kampf, J. Kaplon, V. Karjavin, V. Kekelidze, A. Khudyakov, Yu. Kiryushin, K. Kleinknecht, A. Kluge, M. Koval, V. Kozhuharov, M. Krivda, J. Kunze, G. Lamanna, C. Lazzeroni, R. Leitner, M. Lenti, E. Leonardi, P. Lichard, R. Lietava, L. Litov, D. Lomidze, A. Lonardo, N. Lurkin, D. Madigozhin, G. Maire, A. Makarov, I. Mannelli, G. Mannocchi, A. Mapelli, F. Marchetto, P. Massarotti, K. Massri, P. Matak, G. Mazza, E. Menichetti, M. Mirra, M. Misheva, N. Molokanova, M. Morel, M. Moulson, S. Movchan, D. Munday, M. Napolitano, F. Newson, A. Norton, M. Noy, G. Nuessle, V. Obraztsov, S. Padolski, R. Page, T. Pak, V. Palladino, A. Pardons, E. Pedreschi, M. Pepe, F. Petrucci, R. Piandani, M. Piccini, J. Pinzino, M. Pivanti, I. Polenkevich, I. Popov, Yu. Potrebenikov, D. Protopopescu, F. Raffaelli, M. Raggi, P. Riedler, A. Romano, P. Rubin, G. Ruggiero, V. Ryjov, A. Salamon, G. Salina, V. Samsonov, E. Santovetti, G. Saracino, F. Sargeni, S. Schifano, V. Semenov, A. Sergi, M. Serra, S. Shkarovskiy, A. Sotnikov, V. Sougonyaev, M. Sozzi, T. Spadaro, F. Spinella, R. Staley, M. Statera, P. Sutcliffe, N. Szilasi, M. Valdata-Nappi, P. Valente, B. Velghe, M. Veltri, S. Venditti, M. Vormstein, H. Wahl, R. Wanke, P. Wertelaers, A. Winhart, R. Winston, B. Wrona, O. Yushchenko, M. Zamkovsky, A. Zinchenko.

PoS(QFTHEP 2013)035

1. Introduction

The main aim of the NA62 experiment is to measure precisely the branching ratio of a very rare decay $K^+ \to \pi^+ \nu\bar{\nu}$, which is sensitive to new physics [1] via loop processes and is predicted with high precision in the frameworks of Standard Model (SM) [2]. The NA62 plans to improve the current experimental precision [3] $\mathrm{BR}(K^+ \to \pi^+ \nu\bar{\nu}) = (1{,}73^{+1{,}15}_{-1{,}05}) \times 10^{-10}$ exploiting a novel decay-in-flight technique based on calorimetry to veto extra particles, very light mass trackers to reconstruct the K^+ and the π^+ momenta and full particle identification capability.

2. Detectors

The detector elements are listed here together with a brief functional description. Full detail can be found in the NA62 Techinal design document [4]. The composition and layout of beam and detectors are inspired by the experience gained with the previous kaon decay experiment NA48 performed at the CERN SPS. A secondary kaon beam line, $\approx$ 100m long, leads to a $\approx$ 65 long fiducial region, followed by a further volume, over which the kaon decay products fly apart with respect to the beam line, so that they can be recorded in a series of detectors surrounding the beam.

The overall beam and detector layout is shown in Fig. 1:

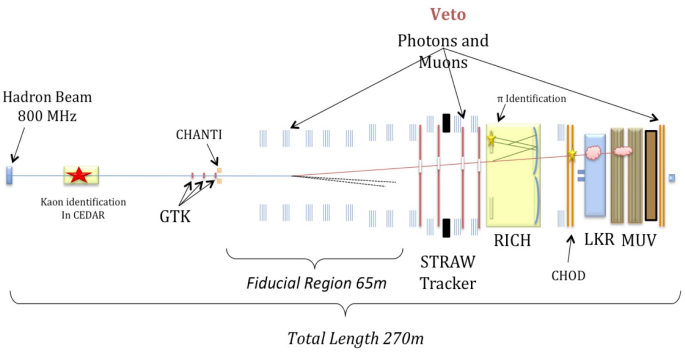

Figure 1: Layout of the NA62 detector.

1. the CEDAR is upgraded differential Cherenkov counter (CEDAR) [**?**], placed on the incoming beam to identify the K^+ component of the beam;

2. The GIGATRACKER (GTK) is comprised of three Si micro-pixel stations measuring time, direction and momentum of the beam particles before entering the decay region;

3. The STRAW TRACKER measures the coordinates and momentum of secondary charged particles originating from the decay region. To minimise multiple scattering the chambers are built of ultra-light material and are installed inside the vacuum tank;

4. The RICH detector is a gas Ring Imaging Cherenkov counter, providing muon/pion separation in the momentum range between 15 and 35 GeV/c;

5. A system of Photon-Veto detectors provides hermetic coverage from zero out to large (∼50mrad) angles from the decay region. This is assured by the existing high-resolution Liquid Krypton electro-magnetic calorimeter (LKR), by Intermediate Ring (IRC) and Small-Angle (SAC) Calorimeters at small and forward angles and by a series of 12 annular photon-veto (LAV) detectors (LAV) at large angles;

6. The Muon-Veto Detectors (MUV) are composed of a two-part hadron calorimeter followed by additional iron and a transversally-segmented hodoscope. This system detects and rejects the muons;

7. These detectors are complemented by 'guard-ring' counters (CHANTI) surrounding the last GTK station, and the charged-particle hodoscope (CHOD), covering the acceptance and located between the RICH and the LKR calorimeter;

8. All these detector are operated and inter-connected with a high-performance trigger and data-acquisition (TDAQ) system.

3. Experimental Strategy

The two undetectable neutrinos in the final state require the design of an experiment with redundant measurement of the event kinematics and hermetic vetoes to achieve a background rejection S/B $\simeq$10. Particular care has to be taken to suppress the two-body decays $K^+ \to \pi^+\pi^0$ and $K^+ \to \mu^+\nu$ which have branching ratios up to 10^{10} times larger than the expected signal. The reconstruction of the two body kinematics may suffer from reconstruction with "non-Gaussian tails", and backgrounds can originate if photons from $K^+ \to \pi^+\pi^0$ are not detected or if muons from $K^+ \to \mu^+\nu$ are mis-identified as pions. To suppress backgrounds from the two body decays, kinematics and Particle Identification (PID) have to be used in conjunction. Backgrounds from K^+ three- and four-body decays are also potentially dangerous. For convenience the most frequent K^+ decay modes are written in Table 1, where they are reported together with the techniques intended to reject them.

Decay Mode	Branching Ratio	Background Rejection
$K^+ \to \mu^+\nu$	64% (called $K_{\mu 2}$)	μ PID, Two-Body Kinematics
$K^+ \to \pi^+\pi^0$	21%	Photon Veto, Two-Body Kinematics
$K^+ \to \pi^+\pi^+\pi^-$	7%	Charged Particle Veto, Kinematics
$K^+ \to \pi^0\mu^+\nu$	3,4% (called $K^+_{\mu 3}$)	Photon Veto,μ PID
$K^+ \to \pi^0 e^+\nu$	5,1% (called K^+_{e3})	Photon veto, E/p

Table 1: The most frequest K^+ decay modes.

Two acceptance regions can be defined to be kinematically free from most of the frequent kaon decays. The kinematic of the decay under study is schematically sketched in Fig. 2, where the momentum of the incoming kaon P_K, the momentum of the outgoing pion P_π and the angle between the mother and the daughter particle, $\theta_{\pi K}$ are the only measurable quantities. It is convenient to use

the squared missing mass variable, m^2_{miss}, defined under the hypothesis that the detected charged particle in the final state is a pion:

$$m^2_{miss} \simeq m^2_K(1-\frac{|P_\pi|}{|P_K|})+m^2_\pi(1-\frac{|P_K|}{|P_\pi|})-|P_K||P_\pi|\theta^2_{\pi K}. \tag{3.1}$$

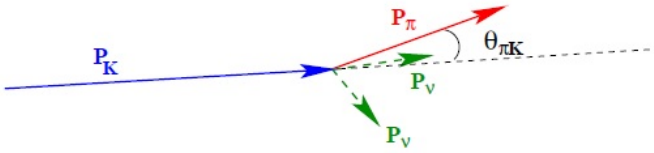

Figure 2: Kinematics of the decay under study.

In Fig. 3 the m^2_{miss} for the signal and the kaon decays with the largest branching ratios are shown for P_K = 75 GeV/c. If resolution effects are ignored, the $K^+ \to \pi^+\pi^0$ decay is constrained to a line at $m^2_{miss} = m^2_{\pi^0}$; the m^2_{miss} of the three-pion decays shows a lower boundary. The m^2_{miss} of $K_{\mu 2}$ does not appear as a line at $m^2_{miss} = 0$ because it is wrongly evaluated, under the assumption that the track is a pion. For this decay the shape depends on the momentum of the particle in the final state and has $m^2 = 0$ as the upper boundary. In conclusion, about 92% of the kaon decays are kinematically limited and their rejection relies on the reconstruction of the kinematics.

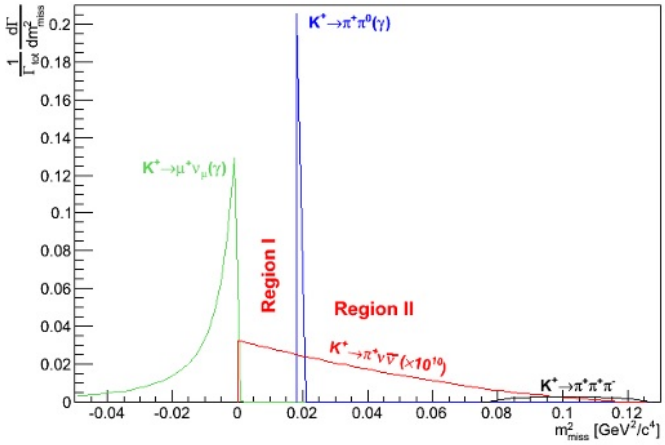

Figure 3: Distribution of the missing mass squared for the signal and the most frequent kaon decays.

Because the peak of the $K^+ \to \pi^+\pi^0$ decays lies within the signal region, we are forced to divide the signal acceptance into two different regions:

- Region I: $0 < m^2_{miss} < m^2_{\pi^0} - (\Delta m)^2$
- Region II: $m^2_{\pi^0} + (\Delta m)^2 < m^2_{miss} < \min m^2_{miss}(\pi^+\pi^+\pi^-) - (\Delta m)^2$

The Δm term depends on the m^2_{miss} resolution and define the required performance of the upstream and downstream spectrometer, namely the Gigatracker and the Double Spectrometer.

A critical aspect of the experiment is that the high rate in the Gigatracker can lead to a situation in which a pion track measured in the downstream spectrometer is wrongly associated to a kaon candidate in the Gigatracker. When this happens, the kinematical rejection power is degraded. To avoid the combinatorial background, a very good time resolution of the Gigatracker is essential.

Semi-leptonic and radiative decays can populate the acceptance region because the kinematics do not constrain them.

In order to suppress all K^+ decay modes that might fake the $K^+ \to \pi^+ \nu\bar{\nu}$ signal, it is necessary to render the detector hermetic with respect to photons from π^0 originating in the K^+ fiducial decay region. This can be provided, in order of increasing angular coverage, by a forward SAC, IRC, LKR and, finally, 13 Large Angle Photon Veto counters (covering angles out to ≈ 50 mr).

There also exist decay modes (with branching ratios $\geq 10^{-5}$), e.g. K_{e4} ($K^+ \to \pi^+\pi^- e^+ \nu$) and $K^+_{\mu 4}$), in which the e^+ (μ^+) may escape detection. By analogy to the case of decays to π^0, it is mandatory that the π^- be observed and that the detector therefore be rendered hermetic with respect to negatively charged particles of momentum ≤ 60 GeV/c. This function can most readily be provided by the straw detectors, which form the active elements of a Double Magnetic Spectrometer.

4. Results from the 2012 Technical Run(TR)

Fig. 4 shows the comparison between the detector used in the TR and the final layout of the experiment. There were installed the following detectors: CEDAR, KTAG, CHANTI, STRAW Chamber 1 with two Modules, eight LAV detectors, CHOD/NHOD, LKR, MUV2 and MUV3, SAC, 85 m (out of 115 m in total) vacuum tank and corresponding detector elements, the primary pumping system and three (out of seven) cryopumps.

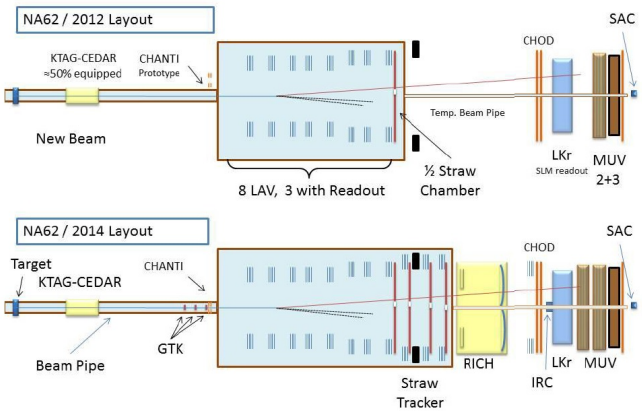

Figure 4: Schematic comparison of the detector layout used in the TR and the final layout.

The TR took place from October 29 to December 3, 2012 and shifts were run around the clock during the 5-week period.

The test of the response of the sub-detector systems using pure kaon decays was an important goal of the 2012 NA62 TR. The analysis aims to select $K^+ \to \pi^+\pi^0$ events. Such a sample gives the possibility to test the response of the detectors to pions and photons, to study the timing correlation between the sub-detectors and to investigate the related activity in the veto detectors, namely the LAV stations and the MUV3. The analysis makes use of the data collected during a short data taking run. The trigger requested: an energy deposition in the Neutral Hodoscope (NHOD) and at least one coincidence (Q1) between two quadrants of the Charged Hodoscope (CHOD). The first condition tagged events with an energy deposition in the LKr calorimeter without using any information from the ionization signal of the LKr itself; the second condition selected events with at least one track in the detector acceptance. The CEDAR, two stations of LAV, the CHOD, the LKr, the MUV2 and the MUV3 were readout in this run. The CEDAR was tuned to detect only the Kaons. The average beam intensity was $\sim 10^{10}$/s (1/50 of the full one). About 8×10^6 triggers have been collected in this run subdivided in about 450 bursts. About 10% of bursts have been rejected because of data corruption due to readout problems. In order to test the LKR performance, the selection scheme is the following:

- identification of at least two clusters in the LKr compatible with an electromagnetic-like energy deposition;
- reconstruction of the π^0 four-momentum by looking at all the possible decay vertecies of the event formed by each pair of LKr clusters in the hypothesis of the π^0 mass;
- reconstruction of the π^+ by using the π^0 four-momentum previously reconstructed and the K^+ four-momentum defined at the percent-level by the beam constraint itself.

As a result the $K^+ \to \pi^+\pi^0$ events exhibit a peak in the missing mass distribution, $m^2_{miss} = (P_K - P_{\pi^0})^2$, corresponding to $m^2_{\pi^0}$.

The analysis of the data from one run collected by NA62 during the technical run allows the selection of a pure sample of more than 4×10^4 $K^+ \to \pi^+\pi^0$ with a percent level background (Fig. 5). A clear timing correlation is present between the various subdetectors, showing time resolutions for the LKr, the CEDAR, the CHOD and the MUV3 below 500 ps. The efficiency of the CEDAR, CHOD and MUV2 are well under control. The measured inefficiencies are in agreement with the expectations and are mostly linked to the partial configuration of the detectors and readout system adopted during the run. The out-of-time activity in the LKr and MUV3 due to the beam seems also in agreement with the expectations. The $K^+ \to \pi^+\pi^0$ is not suitable for measuring the efficiency of the LAVs and the MUV3. They are under study using different methods together with the accidental activity in the LAV stations. The CHOD and MUV3 provide a sample of muons, useful to highlight the LKr capabilities in detecting MIPs. This also allows an estimation of the expected rate at full intensity in the hottest region of the LKr.

Though the detector construction is still on-going and numerous technical challenges are still in front of the NA62 Collaboration, it is realistic to install the remaining detectors for a first physics run starting in October 2014.

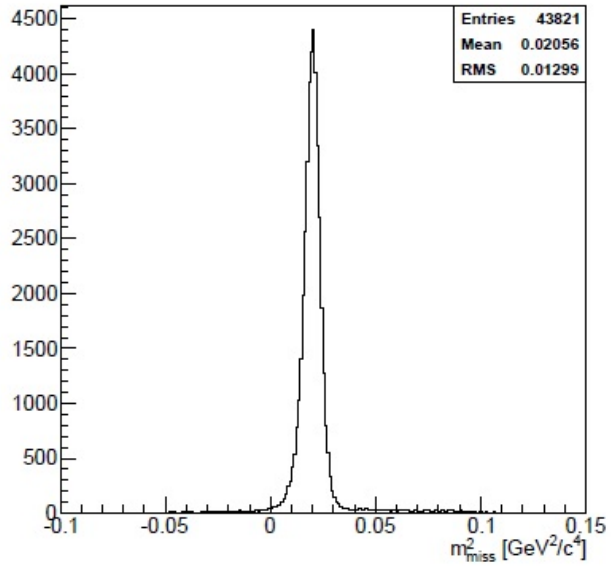

Figure 5: Distribution of the m^2_{miss} for the events, selected after all the cuts.

References

[1] A. Crivellin, L. Hofer, U. Nierste and D. Scherer, *Phenomenological consequences of radiative flavor violation in the MSSM*, *Phys. Rev.* **D84** (2011) 035030 [arXiv:1105.2818 [hep-ph]].

[2] J. Brod, M. Gorbahn and E. Stamou, *Two-Loop Electroweak Corrections for the $K \to \pi\nu\bar{\nu}$ Decays*, *Phys. Rev.* **D83** (2011) 034030 [arXiv:1009.0947 [hep-ph]].

[3] A. V. Artamonov *et al* [BNL-E949 Collaboration], *Study of the decay $K^+ \to \pi^+ \nu\bar{\nu}$ in the momentum region $140 \leq P(\pi) \leq 199$ MeV/c*, *Phys. Rev.* **D79** (2009) 092004 [arXiv:0903.0030 [hep-ex]].

[4] NA62 Technical Design Document, NA62-10-07; https://cdsweb.cern.ch/record/14049857.

[5] S. ANVAR,*et al* [NA48 COLLABORATION], *The Beam and Detector for the NA48 neutral kaon CP violation experiment at CERN*, *Nucl. Instrum. Methods* **A574** (2007) 433.